



Diphenyl triazine hybrids inhibit α -synuclein fibrillogenesis: Design, synthesis and *in vitro* efficacy studies



Mudasir Maqbool^a, Joshna Gadhavi^b, Pravin Hivare^b, Sharad Gupta^{b, **},
Nasimul Hoda^{a, *}

^a Drug Design and Synthesis Lab., Department of Chemistry, Jamia Millia Islamia, Jamia Nagar, New Delhi, 110025, India

^b Biological Engineering, Indian Institute of Technology Gandhinagar, Palaj, Gandhinagar, Gujarat, India

ARTICLE INFO

Article history:

Received 16 May 2020

Received in revised form

13 July 2020

Accepted 28 July 2020

Available online 22 August 2020

Keywords:

Neurodegeneration

Parkinson's disease

Protein aggregation

Drug design

Synthesis

Diphenyltriazine

ABSTRACT

Aggregation of α -synuclein (α -syn) is one of the central hypotheses for Parkinson's disease (PD), therefore, its inhibition and disaggregation is an optimistic approach for the treatment of PD. Here, we report design, synthesis and *in-vitro* efficacy studies of a series of diphenyl triazine hybrids as potential inhibitors of α -syn fibrillogenesis. From the docking studies, we concluded that compounds **A1**, **A2**, **A4**, **A8** and **A9** display promising binding affinity with the essential residues of α -syn with binding energy values: -6.0 , -7.0 , -6.3 , -6.6 and -6.7 kcal/mol respectively. The target compounds were synthesized using multistep organic synthesis reactions. Compounds **A1**, **A2**, **A4**, **A8** and **A9** showed a significant lowering of the α -syn fibril formation during Thioflavin-T assay and fluorescence microscopy. In addition, these compounds **A1**, **A2**, **A4**, **A8** and **A9** also proved to be good disaggregators in the pre-aggregated form of α -syn. Most of the compounds exhibited no cytotoxicity in mouse embryonic fibroblast (MEF) and human adenocarcinomic alveolar basal epithelial cells (A549) except **A2**. Overall, diphenyl triazine-based compounds can be further investigated for the treatment of synucleinopathies and for Lewy body dementia in which α -syn is predominantly observed.

© 2020 Elsevier Masson SAS. All rights reserved.

1. Introduction

Parkinson's disease (PD) is the second most common neurodegenerative disorder after Alzheimer's Disease (AD) which primarily occurs due to the loss of dopaminergic neurons in the substantia nigra region of the brain [1]. The two major pathological hallmarks of PD are Lewy bodies and Lewy neurites in which α -synuclein (α -syn) protein has been found to be the major constituent [2]. α -Syn is 140 amino acid residues long which is a natively unfolded in solution and plays a pivotal role in vesicle trafficking [3,4]. Aggregation of α -syn is one of the central events in the onset and progression of PD and hence *in-vitro* aggregation is extensively used as a model system to study PD [5]. α -Syn aggregation is a multi-step process following nucleation dependent aggregation kinetics that undergoes various stages of aggregation such as nuclei, oligomers, proto-fibrils, fibrils and larger aggregates [6].

Presence of some of these conformers has been confirmed in the diseased brain tissues as well [7]. Therefore, robust inhibitors that could not only avert the fibrillization of α -syn but also disaggregate formerly accumulated aggregates of α -syn in the human brain continue to be an active field of investigation. Researchers have reported different synthetic and natural products that can constrain α -syn aggregation and ameliorate the aggregation associated toxicity [8–10].

1,2,4-triazine based compounds were found to be proficient in penetrating BBB and advantageous agents for preventing neurodegenerative diseases like AD [11,12]. Such compounds were also found to be neuroprotective [13]. In our efforts towards the development of potent multitarget ligands for the treatment of AD, a series of triazine-triazolopyrimidine hybrids was reported that effectively inhibited $A\beta_{42}$ peptide aggregation by 1–1.4 folds better as compared to the effect of curcumin [14]. One more series of cyanopyridine-triazine hybrids also showed better inhibitory activity for $A\beta_{42}$ aggregation (1.09–1.5 folds) at 25 μ M compared to the reference compound curcumin [15]. The plausible reason for their remarkable anti-aggregation activity may be due to the presence of core triazine moiety through which the

* Corresponding author.

** Corresponding author.

E-mail addresses: sharad@iitgn.ac.in (S. Gupta), nhoda@jmi.ac.in (N. Hoda).

pharmacophore acquires a nearly planer structure which in turn enables it to fit between the A β sheets and thus produced an A β disaggregating effect [15]. Hydrazinyl-1,2,4-triazines bearing pendant aryl phenoxy methyl-1,2,3-triazole were correspondingly found to inhibit BACE1 (β -secretase) efficiently. Furthermore, these compounds were found to be neuroprotective against A β peptide toxicity [16]. Recently, the multifunctionality of 5,6-diphenyl triazine-thio methyl triazole hybrids for the anti-Alzheimer effect was also evaluated [17]. The easy synthesis of triazine-based compounds by routine chemical reactions and the roughly planer structure of triazine core structure were also the reasons to choose such compounds as α -syn disaggregating agents.

The rationale for designing diphenyltriazine-based compounds for the anti-PD effect is diagrammatically illustrated in Fig. 1.

Keeping the above aspects into consideration, here we have designed and synthesized a series of diphenyltriazine hybrids as persuasive inhibitors of α -syn fibrillation and disaggregating agents for the treatment of PD. The *in-vitro* ability of the synthesized compounds to inhibit α -syn fibrillogenesis was evaluated. The compounds were also tested for their cytotoxicity effects on MEF cell lines and A549 cell lines.

2. Results and discussion

2.1. *In silico* design of diphenyl-triazine based α -syn inhibitors

To develop a potential drug candidate for PD which could inhibit α -syn aggregation, we undertook the structure-based drug design approach. AutoDock Vina version 1.5.6 was used for flexible docking and redocking of the diphenyl triazine-based molecules and the micelle-bound human α -syn (PDB ID 1XQ8). α -Syn is a 140 amino acid long, small and natively unfolded protein which can be divided into three sequential parts: N-terminal amphipathic region containing maximum sequences and three point mutations associated with autosomal dominant early onset PD, the central NAC region which covers the most hydrophobic residues, and the hydrophilic C-terminal.

Autoinhibition of α -syn by the interaction of C-terminus region with the NAC region has been found to prevent fibrillation under normal conditions [18,19]. The C-terminal region of the protein has an essential part in the interaction of protofibrils required for maturation of fibrils [20]. The amino acid residues of α -syn like Tyr125, Tyr133, and Tyr136 present in the hydrophilic tail of the C-terminus of α -syn play a crucial role in its fibrilization process [21,22]. Previously, the binding of ceftriaxone to bovine serum albumin (BSA) has been reported to increase the polarity and hydrophilicity of the C-terminal of the protein, thereby, increasing the compactness of monomeric α -syn and inhibited its fibril formation [18,23]. Consequently, binding of a putative ligand to the C-terminal region should affect the aggregation of α -syn. Even though the protein topology reveals it in a micelle bound state, the unfolded hydrophilic tail (Asp98-Ala140) can be well suited as a docking target [24].

The choice for selecting diphenyl-triazine core moiety was due to its extended conjugate system and the excellent reports of triazine-based molecules as anti-neurodegenerative agents [14,25]. The aromatic systems joined through the combination of flexible and rigid linkers were expected to promote the non-covalent interactions like π - π stacking interaction and H-bonding with the essential residues of α -syn. Compounds containing various hydrogen bond donor and acceptor groups appeared favorable for their binding with the protein. The docking results provided the approximate binding affinity ($-\Delta G$ in Kcal/mol) between the ligands (**A1–A9**) and the micelle-bound human α -syn that mimics a membrane imbedded conformation as mentioned in Table 1. The

alkyl or aralkyl groups with varying hydrophobicity and electronic properties also dictated the binding affinity of the ligands to the drug target. The binding free energy of the top five compounds **A1**, **A2**, **A4**, **A8** and **A9** with α -syn was found to be -6.9 , -7.2 , -6.6 , -7.0 and -6.7 kcal/mol, respectively which suggest a very high binding affinity between the ligands and the target protein. PyMOL viewer was used for the analysis of the docked structures. From the interpretation of the docking results as shown in Fig. 2A, compound **A1** was found to participate in π - π interaction between chloroquinoline system and Tyr136. Same way, one of the biphenyl rings attached to the triazine core structure was found to interact with Tyr125. From Fig. 2B, we came to know that, biphenyl and triazolopyrimidine systems of **A2** displayed π - π stacking with Tyr125 and Tyr136, the key residues of the protein, respectively. The biphenyl rings attached to the triazine were found to show π - π interaction with Tyr125, simultaneously (Fig. 2C). In the same manner, **A8** displayed a non-covalent interaction with Tyr125. Also, H-bonding interaction of the range of 1.8 Å was observed between the nitrogen of phenylacetamide of **A8** and Met127 (Fig. 2D). In addition to π - π interaction between the aromatic groups of **A9** and Tyr125 and Tyr136, a strong H-bond was detected between the oxygen of phenylacetamide and hydrogen of Ser129 (Fig. 2E).

Bolded values represent the most active binding compounds: **A1**, **A2**, **A4**, **A8** and **A9**.

2.2. Chemical synthesis

The target molecules were synthesized *via* multiple steps as represented in Scheme 1. In the first step benzil (**1**) was made to couple with thiosemicarbazide (hydrazinecarbothioamide) (**2**) in water and ethanol in equal proportions to get **3** according to the reported literature [27]. The compound **3** was treated with 2-chloroacetic acid to get compound **4**. Peptide coupling of compound **4** with different piperazine containing nucleophiles in presence of DMSO as a reaction solvent, triethylamine as base and HBTU as coupling reagent was the final step of the reaction to obtain the target molecules (**A1–A9**). The column chromatography technique was used for the purification of all the molecules and the purified compounds were characterized by ^1H NMR, ^{13}C NMR, ESI MS and elemental analysis.

2.3. *In-vitro* evaluation of the designed and synthesized compounds (A1–A9) as α -syn aggregation inhibitors

2.3.1. Expression and purification of α -Syn protein and its characterization

Recombinant tag-free α -syn was overexpressed in *Escherichia Coli* BL21 (DE3), and since the protein is primarily localized in the periplasm, the osmotic shock method was used to extract the protein as described previously [28]. Further purification of α -syn was carried out on DEAE (Diethyl aminoethyl)-Sephacel, an anion exchange matrix column, using a gradient elution of NaCl with concentration changing from 50 mM to 500 mM. As shown in Fig. 3a, SDS-PAGE analysis of various fractions revealed that the purified protein was primarily present in 300–500 mM NaCl fractions. All these fractions were pooled and dialyzed against water to yield a salt-free preparation of α -syn with purity >95% as kinetics of fibrillization of α -syn is sensitive to the identity and concentration of salts present [29]. To further ensure the monomeric nature of α -syn before each assay, the salt free protein was first dissolved in base and then acidified to a neutral pH. This was followed by a high-speed centrifugation at 100,000 g to remove any residual aggregates. Above steps were necessary to obtain a consistent and baseline kinetic aggregation profile for comparing the inhibitory effect of synthesized compounds. The identity of purified α -syn was

further confirmed by Western blot using H3C monoclonal antibody which gave a single band with M.Wt. ~17 kDa, as shown in Fig. 3b. This was higher than theoretical M.Wt. ~14.4 kDa, due to low binding of acidic C-terminal region of α -syn to SDS as observed previously [28].

2.3.2. *In vitro* monitoring of α -syn fibrillization in the presence of inhibitory compounds (A1-A9)

Thioflavin T (ThT) is a benzothiazole based dye that exhibits several-fold enhancements in the fluorescence emission upon binding to the cross β -sheet structures, a hallmark of amyloids and hence is widely used to monitor the *in vitro* aggregation in real-time [30]. The progress of α -syn aggregation (70 μ M) was monitored in the presence of ThT at 37 °C by capturing fluorescence emission at 485 nm (excitation at 445 nm) in a microplate spectrofluorometer. A sigmoidal ThT fluorescence curve was obtained for α -syn aggregation with a distinct lag phase preceding the growth phase, followed by a plateau phase mimicking a typical nucleation dependent fibrillization kinetics. To test the inhibitory potential of synthesized compounds (A1-A9) α -syn aggregation was carried out in PB, pH 7.4 supplemented with the inhibitors dissolved in DMSO, such that the final concentration of DMSO was 10% (v/v) and α -syn to inhibitor molar ratio was fixed at 1:1. As a positive control, DMSO sans any inhibitory compounds was added to the aggregation mixture. As shown in Fig. 4, while there was no

apparent lengthening of the lag phase, all compounds A1-A9 caused a decline in the final plateau fluorescence (F_{final}) to varying extents. Although F_{final} does not relate absolutely to the amount of amyloid formation, a relative measure of β -sheet rich structures formed could be inferred and we relied on the % decline in the F_{final} to compare the inhibitory potential [31,32]. A significant decrease would indicate that a particular compound can inhibit the fibrillization under the given aggregation reaction conditions. As shown in Fig. 5, A1, A2, A8 and A9 significantly inhibited α -syn fibrillization as indicated by more than 50% decline in F_{final} ($p < 0.01\%$). These compounds were also top scorers according to our computational predictions based on docking studies (Table 1). A3, A4, and A7 also exhibited significant lowering ($P < 0.05$) but decline was less than 40% in F_{final} . To rule out any interference due to self-aggregation of the inhibitory compounds, A1-A9 were separately incubated with ThT only in the absence of α -Syn for more than 2 weeks but no change in ThT fluorescence was observed (data not shown).

To gain further insights into the mechanism of inhibition by A1-A9, we calculated lag-time (t_{lag}), time required to reach halfway through the elongation phase ($t_{1/2}$) and apparent elongation rate constant K_{app} for the growth of fibrils from ThT fluorescence sigmoidal curve [33]. As shown in Table 2, except A2, no significant change in t_{lag} or $t_{1/2}$ was observed when compared to uninhibited fibrillization reaction. This indicates that compounds are probably inhibiting the elongation phase with no significant impact on

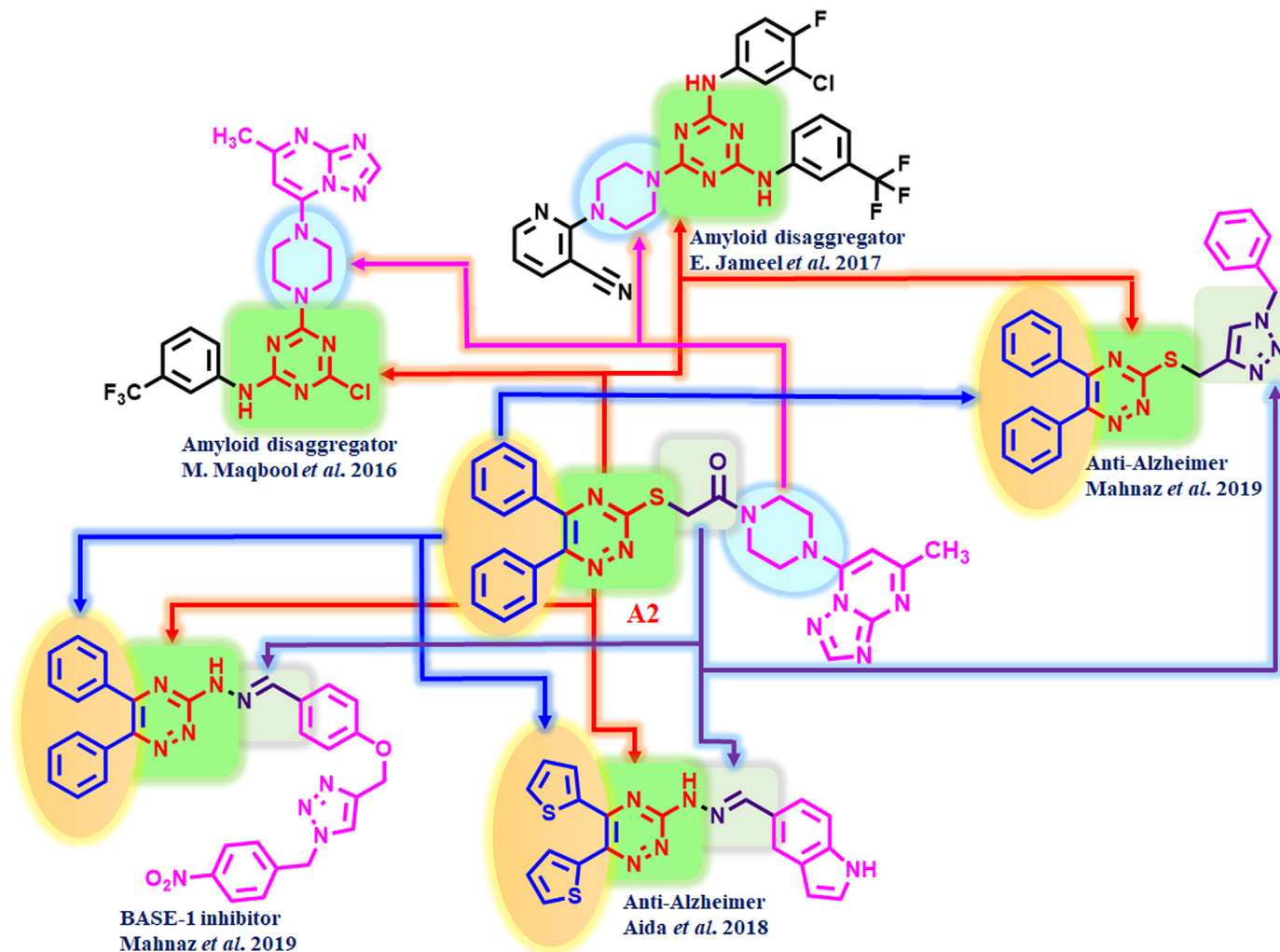


Fig. 1. The rationale for the design of diphenyltriazine analogues for inhibiting α -syn fibrillogenesis.

Table 1

The calculated binding free energies of the selected derivatives in molecular docking using Auto Dock Vina [26].

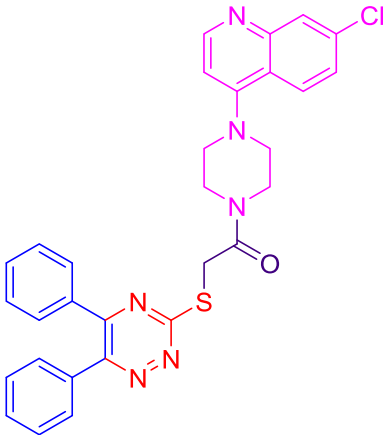
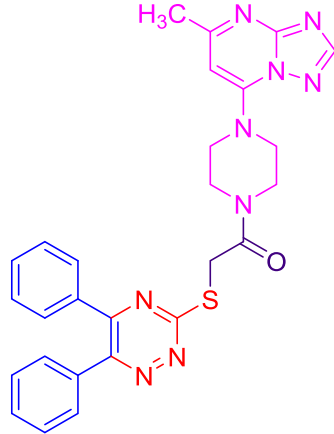
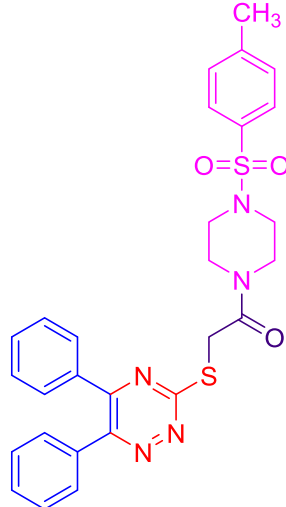
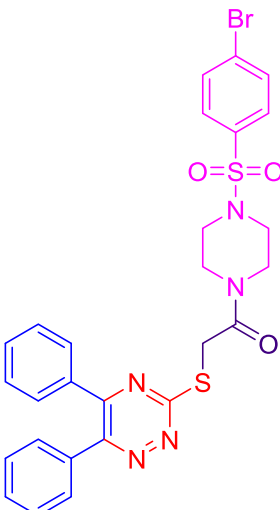
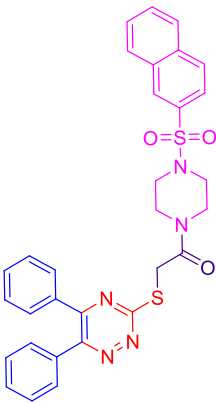
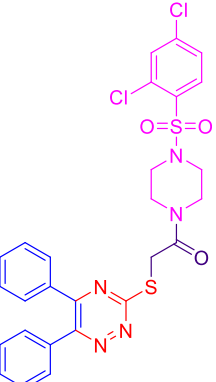
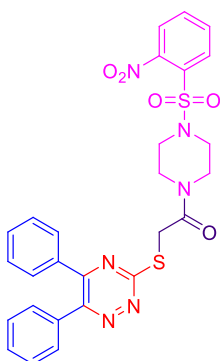
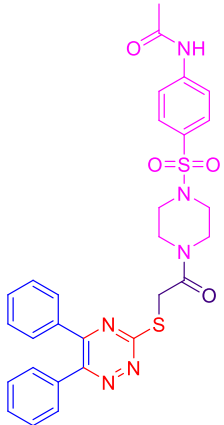
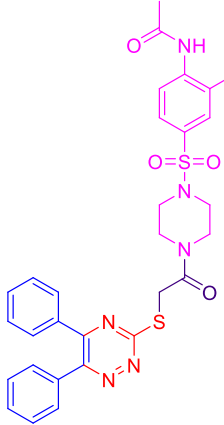
Compound name	Compound structure	Binding affinity (kcal/mol)
A1		-6.9
A2		-7.2
A3		-6.1

Table 1 (continued)

Compound name	Compound structure	Binding affinity (kcal/mol)
A4		-6.6
A5		-6.0
A6		-6.4

(continued on next page)

Table 1 (continued)

Compound name	Compound structure	Binding affinity (kcal/mol)
A7		-5.4
A8		-7.0
A9		-6.7

nucleation or early aggregation. **A2** appeared to be the exception as initial acceleration leading to an earlier onset of elongation phase was observed. F_{final} for **A1** and **A2** was nearly identical which suggested a similar role of bulkier bicyclic ring system on inhibition of α -syn aggregation. **A8** appear to have accelerated the fibrillization process but overall β -sheet levels remained lower indicated by low F_{final} . Additionally, only **A8** showed a significant decrease in K_{app} which pointed to its interference in proto-fibril formation or fibrillization process.

From the above analysis it appears that compounds could suppress fibrillization to a certain extent acting as thermodynamic inhibitors only [32]. Here, it is important to note that we have used only a 1:1 M ratio of protein to inhibitor, and since inhibitors could

also bind to regions other than non-amyloidogenic which in turn could reduce the inhibitory potential during the early stages of aggregation. However, as the aggregation proceeds, the stoichiometric ratio favors inhibitors and the further extension of the protofibrils/fibrils is stalled prematurely resulting in lower F_{final} than positive control. A logical step would have been to use a higher concentration of the inhibitors but we were limited by the solubility of the compounds in aqueous aggregation buffer. Similarly reducing the concentration of α -syn to tip the stoichiometric ratio towards inhibitor could not be practiced as a mere two-fold drop in the concentration, lengthens the aggregation kinetics to nearly three weeks.

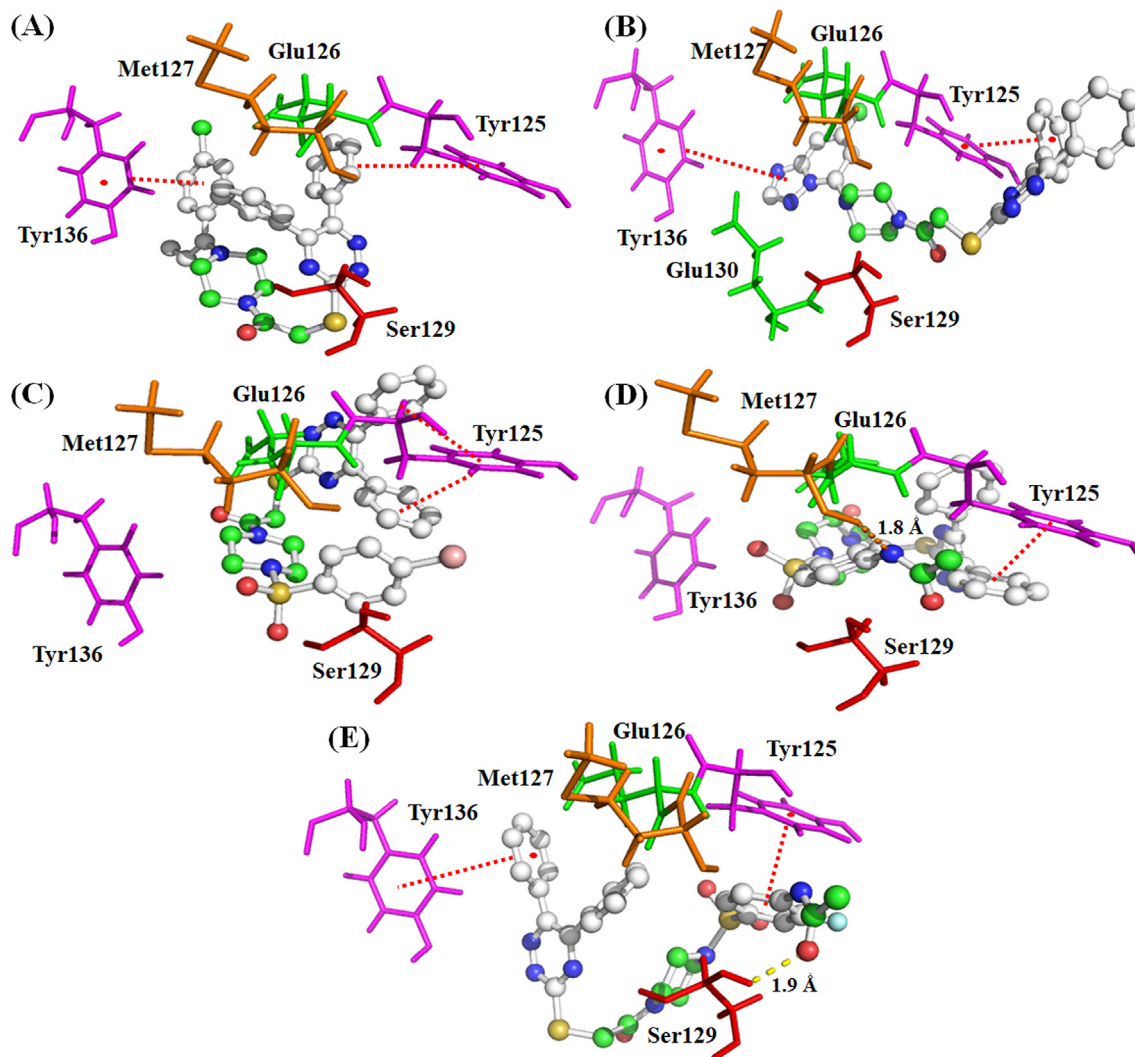


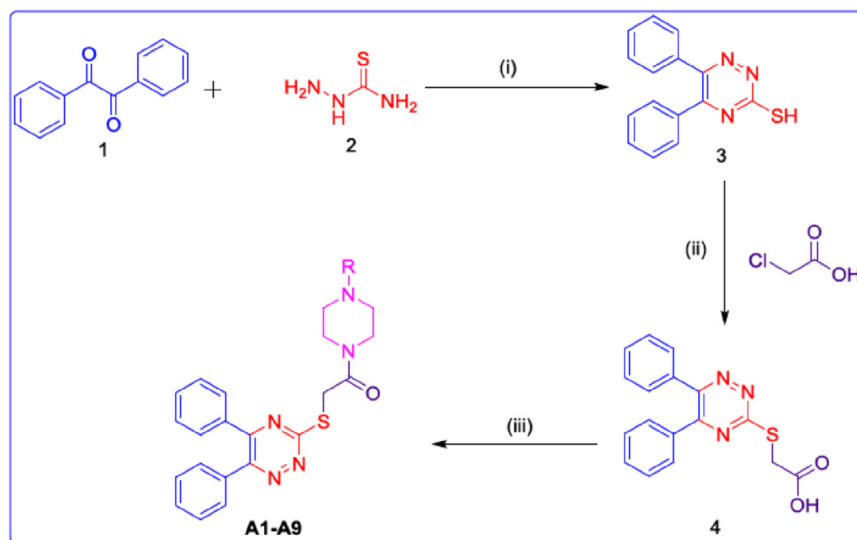
Fig. 2. Molecular interaction of compounds **A1**, **A2**, **A4**, **A8** and **A9** with α -syn (PDB ID 1XQ8). (A) Binding interactions of compound **A1** with α -syn. (B) Molecule **A2** in the binding pocket of α -syn. (C) **A4** in the binding pocket of α -syn. (D) Interaction between the essential residues of α -syn with **A8** compound. (E) **A9** with C-terminus residues of α -syn. Tyr is shown in magentas, Met in orange, Glu in green and Ser in red colours. H-bonding and π - π interactions are shown with yellow and red coloured dotted lines respectively. PyMOL viewer was used for the analysis of the docked structures. (For interpretation of the references to colour in this figure legend, the reader is referred to the Web version of this article.)

2.3.3. Fluorescence microscopy imaging of inhibition of α -syn fibrillogenesis and disaggregation

Based on ThT fluorescence results, we selected **A1**, **A2**, **A8** and **A9** for further evaluation as they exhibited significant inhibition ($p < 0.01$). Additionally **A4** was chosen based on docking results and moderate inhibition ($p < 0.05$) by ThT fluorescence assay. After the completion of the assay (≥ 66 h) aggregated samples (control as well as inhibited) were observed under the fluorescence microscope. Since ThT was already bound to fibrils and had become fluorescently active, no additional dye was required and the samples could be directly visualized through FITC filter. Representative images are shown in Fig. 6. As expected, uninhibited α -syn sample displayed abundant brightly illuminated fibrous structures (Fig. 6a). In the case of **A2**, only a very few ThT positive aggregates were visible. **A4** and **A8** also appear to be effective in lowering the density of fluorescently illuminated aggregates but **A1** and **A9** were only moderately effective. Considering the heterogeneity of the aggregated samples it was not feasible to do a quantitative analysis but the reduction in fluorescently labelled aggregates was clearly visible when imaged at a lower zoom level covering a much larger area.

Some studies have suggested that ThT could be knocked off in the presence of inhibitors leading to a lower fluorescence value or false negatives under the fluorescence microscope [34]. Hence, we added more ThT to the mixture to ensure that any unlabelled aggregate are also illuminated and collected the images again. The images before (i.e. directly from the sample well) and after adding ThT were qualitatively similar which supported our earlier observations about inhibitory potentials of compounds.

While several small molecules can inhibit α -syn aggregation only a few have the ability to disaggregate preformed α -syn fibrils. To further test if **A1**, **A2**, **A4**, **A8** and **A9** can also disaggregate previously formed aggregates, we incubated α -syn fibrillary aggregates (formed in the absence of ThT and any inhibitor) in the presence of the compounds at 37 °C for a period of 5 days in the same (1:1) α -syn to inhibitor molar ratio as used earlier. After adding ThT, the samples were observed under the fluorescence microscope through FITC filter (see Fig. 7). While the control α -syn sample was populated with brightly illuminated fibrous aggregates expectedly, samples incubated with **A1**, **A2**, **A8** and **A9** had sparsely populated, dimly lit aggregates only indicating that these compounds were also effective disaggregators. However, **A4** was not able to dissolve



Reagents and conditions

(i) Ethanol:water=1:1, 80 °C, 18 h (ii) Acetone, Et₃N, 60 °C, 4h (iii) Et₃N, HBTU, DMSO, rt, 24 h.

Compound (A1–A9)	R
A1	4,7-dichloroquinoline
A2	7-chloro-5-methyl-[1,2,4]triazolo[1,5-a]pyrimidine
A3	4-methylbenzenesulfonyl chloride
A4	4-bromobenzenesulfonyl chloride
A5	naphthalene-2-sulfonyl chloride
A6	2,4-dichlorobenzenesulfonyl chloride
A7	2-nitrobenzenesulfonyl chloride
A8	4-acetamidobenzenesulfonyl chloride
A9	4-acetamido-3-fluorobenzenesulfonyl chloride

Scheme 1. Synthesis of diphenyl triazine-based compounds.

pre-formed fibrils as the corresponding images were qualitatively similar to the control samples.

Based on the above evidences we deduced that α -syn aggregation inhibition is sensitive to variation of substitution to the diphenyltriazine moiety. We further tried to correlate the nature of the substituent with the inhibitory potential of the compounds A1–A9. Here, A2 appeared to be the most promising inhibitor which not only showed the highest affinity towards α -syn upon docking but was also the best *in situ* inhibitor as well as disaggregator. This was probably due to higher affinity of the fused triazole-pyrimidine group towards α -syn perhaps due to added charge-charge interaction.

A3, A5, A6 and A7 contain methylphenyl, naphthalene, dichlorophenyl and nitrophenyl groups attached to the sulphonyl group, respectively which makes them comparatively less bulky and hence the reason for their insignificant role in α -syn disaggregation. Interestingly, A8 and A9 which carry a phenylacetamide group attached to sulphonyl at para position were very effective in inhibiting aggregation as well as dissolving preformed aggregates.

2.3.4. Cytotoxicity evaluation through MTT assay

The cytotoxicity of inhibitor compounds was determined in mouse embryonic fibroblasts (MEF) which is a non-cancerous cell line. The cells were grown in a media containing the compounds (A1, A2, A4, A8 and A9) at concentrations of 10 μ M and cell viability was determined using MTT assay. As a control, we used DMSO which was also used for solubilizing compounds for stock preparation. As shown in Fig. 8, compounds A1, A4, A8 and A9 did not cause any significant toxicity to the cells even after 24 h of treatment. Only A2 appeared to be mildly toxic at 10 μ M. The compounds were further tested against human adenocarcinomic alveolar basal epithelial (A549) cells as shown in supplementary information (Fig. S1). Concentrations as high as 0.4 mM for all the compounds were well tolerated with no significant cytotoxicity except A2 which killed >60% cells at 50 μ M. Thus, barring A2, which incidentally seemed to be the most promising candidates based on docking studies as well as experimental evidence, all other compounds can be safely employed for further assessment of inhibitory potential in cell culture models.

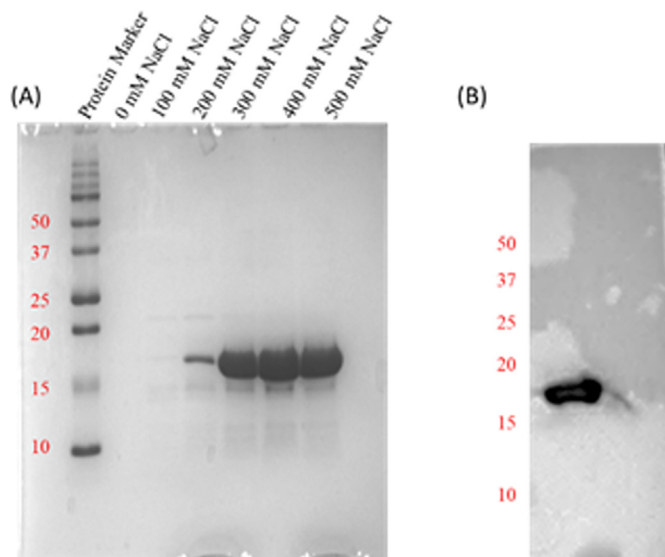


Fig. 3. α -Syn purification and characterization. (A) 15% SDS-PAGE image of purified α -syn fractions eluted in PB buffer using varying NaCl concentration (B) Detection of purified protein by Western blot using α -syn specific monoclonal antibody H3C.

2.3.5. Effect of inhibitors on aggregated α -synuclein cytotoxicity

The cytotoxic behaviour of *in vitro* aggregated α -syn has been well documented in the literature [5]. Any promising inhibitor shall not only lower the aggregate count but also reduce the cytotoxicity associated with aggregated α -syn. Accordingly, the MEF cells were treated with monomeric α -syn, aggregated α -syn and α -syn aggregated in the presence of inhibitors. As shown in the Fig. 9, aggregated α -syn treated with MEF cells, caused a significant decrease in cell viability ($p < 0.05$). The cells incubated with α -syn aggregated in the presence of inhibitors **A1**, **A2** and **A9** also showed a moderate toxic effect on cells. However, the cells incubated with α -syn aggregated in the presence of **A4** and **A8** exhibited no cytotoxicity and appeared to have a protective effect on MEF cells against α -syn aggregates. These findings indicate that **A4** and **A8** not only reduce the aggregation level *in vitro* but also ameliorate any cytotoxicity associated with aggregated α -syn and hence are the prime candidates for further development.

2.3.6. Prediction of BBB permeability and drug likeness

Carrying the lead drug candidates through the blood–brain barrier (BBB) is a major challenge and fate deciding factor for the development of novel neurotherapeutics [35]. Various triazine based compounds having certain similarities in their structure, size and shape with the compounds of the present study have been found to cross BBB. For example, BKM120 (Buparlisib) a triazine cores structure-based brain penetrable pan-PI3K/mTOR inhibitor is clinically used for the treatment of cancer [36]. Similarly, PQR309 (Bimiralisib) is also reported to be orally available, cross the blood–brain barrier, and display favorable pharmacokinetic parameters in mice, rats, and dogs [37].

We used AdmetSAR: a wide-ranging source for calculation of chemical ADMET properties of the compounds [38]. Most of the compounds were found to follow the parameters such as hydrogen bond donors less than 5, hydrogen bond acceptors less than 10, rotatable bonds less than 10, molecular weight less than 750 Da, and $\log P$ less than 10 (Table S1, Supporting information).

In addition, we used BBB predictor developed by Liu *et al.* [39] to confirm whether a compound can cross the BBB (BBB+) or not (BBB-). Lipophilicity ($\log P$), charges, flexibility (rotatable bonds),

hydrogen bond donors and acceptors, size (MW, number of rings) and shape (ovality) descriptors, surface and volume descriptors (hydrophobic, hydrophilic), amphiphilicity, etc were found to be in a range favouring their ability to cross BBB for all compounds tested.

3. Conclusion

In summary, nine new diphenyltriazine derivatives were synthesized and characterized as inhibitors of α -syn fibril formation as well as disaggregators. The compounds were first designed using AutoDock Vina version 1.5.6 and then synthesized using convergent organic synthetic routes. Docking studies revealed that these compounds participate actively in non-covalent interaction with the key residues of the α -syn protein. From *in-vitro* ThT assay, **A1**, **A2**, **A8** and **A9** showed a significant lowering of the α -syn fibril formation even at equimolar ratio which was further confirmed by fluorescence microscopy. These compounds were also the top binders predicted by the docking study and further found to be effective disaggregators of preformed α -syn aggregates. Except **A2** which was moderate cytotoxic, all the compounds were found to have no significant effect on cellular viability. Also **A4** and **A8** appeared to ameliorate cytotoxicity associated with α -syn aggregates.

Overall, we have successfully demonstrated the utility of diphenyl triazine hybrids as inhibitors for α -syn aggregation. These scaffolds could be further tested for efficacy in cellular as well as *in vivo* models of PD treatment.

4. Experimental

4.1. Docking protocol

Crystal structure of α -syn (PDB ID 1XQ8) in pdb format was downloaded from Protein Data Bank (www.rcsb.org) [40]. Auto-Dock Vina version 1.5.6 was used to perform docking with the ligand molecules. During the docking process, the simulation boxes were prepared large enough to cover the interaction residues of the protein and the ligand [26]. PyMOL visualization tool was used to visualize the molecular interactions. Weak non-covalent interactions like π - π stacking interaction and H-bonding were observed between the hydrophilic C-terminus residues of α -syn and the ligand molecules lying within a range of 2.5 Å. In addition, binding free energy was calculated on the basis of which the designed molecules were screened.

4.2. Chemistry

All reagents and solvents were commercially available and used as purchased without further purification. Melting points (mp) were determined on a Stuart Scientific SMP1 apparatus and are uncorrected. Proton nuclear magnetic resonance (^1H NMR) spectra were recorded on a Bruker 300 MHz FT spectrometer. Proton chemical shifts are reported in ppm (TMS, δ 0.00) or with the solvent reference relative to TMS employed as the internal standard (CDCl_3 , δ 7.26; $\text{DMSO}-d_6$ δ 2.54). The multiplicities of NMR signals are designated as s (singlet), d (doublet), dd (double doublet), t (triplet), q (quartet), br (broad), m (multiplet, for unresolved lines). LCMS of the compounds were carried out on applied biosystem (absciex 2000 triple quad). Column chromatography was performed on columns packed with alumina from Merck (60–120 mesh). Aluminum oxide thin-layer chromatography (TLC) cards from Merck (aluminum oxide-precoated aluminum cards with fluorescent indicator detectable at 254 nm) were used for TLC. Developed plates were visualized by a Spectroline ENF 260C/FE UV

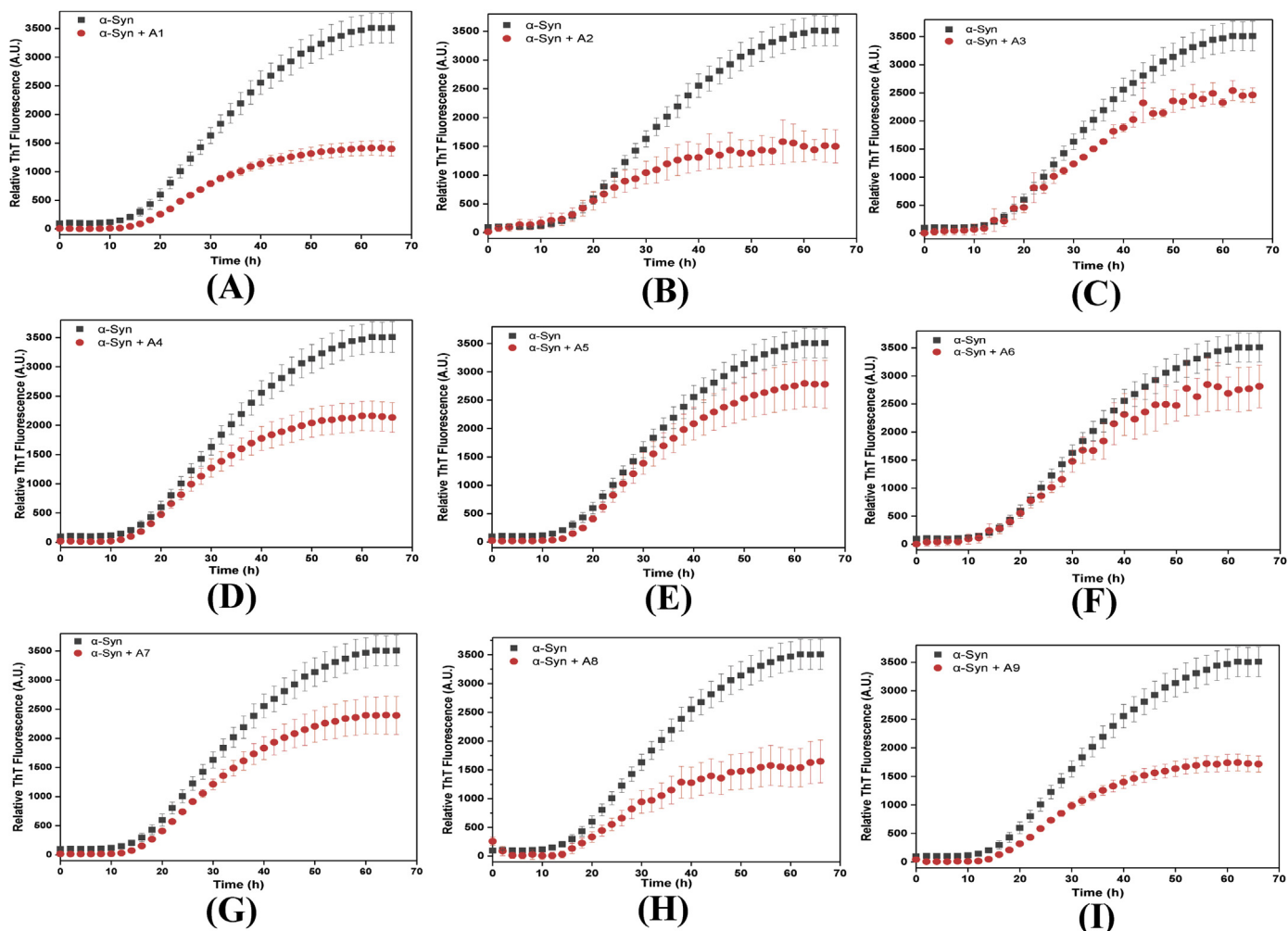


Fig. 4. Time dependent aggregation kinetics for α -syn and α -syn incubated with inhibitors (A1-A9). Each panel (A–I) represents ThT fluorescence (Ex: 440 nm and Em: 485 nm) from aggregation reaction of 70 μ M α -syn in PB buffer supplemented with 10% (v/v) DMSO at 37 $^{\circ}$ C in the absence (black dot) or presence of 70 μ M inhibitor compounds (red dots). Here, each data point represents \pm SEM of fluorescence values from four different wells of three independent replicates. (For interpretation of the references to colour in this figure legend, the reader is referred to the Web version of this article.)

apparatus. Organic solutions were dried over anhydrous sodium sulfate. Evaporation of the solvents was carried out on a Büchi rotavapor R-100 equipped with a Büchi V-100 vacuum controller. Elemental analyses were obtained in an Elementar Vario analyser. Elemental analyses of the compounds were found to be within $\pm 0.4\%$ of the theoretical values. The purity of tested compounds was $>95\%$.

4.2.1. General procedure for the synthesis of compound 3 [27]

Thiosemicarbazide (0.65 g, 7.1 mol) dissolved in 30 mL water was put for regular stirring at room temperature. K_2CO_3 (2 g, 14.4 mol) was added to the stirring solution of thiosemicarbazide. The reaction mixture was allowed for stirring at room temperature for 1 h. Now ethanolic solution of benzil (1.5 g, 7.1 mol) was added to it. The reaction mixture was refluxed at 80 $^{\circ}$ C for 16 h. After the completion of the reaction, the reaction mixture was acidified to pH 3 with acetic acid to obtain a yellow coloured precipitate. The precipitate obtained was filtered and dried and was used for forward reaction steps without any purification.

4.2.2. General procedure for the synthesis of compound 4

Triethylamine (1.7 g, 16.8 mol) was added to a solution of compound 3 (3 g, 11.1 mol) in 30 mL acetone at room temperature.

After 1 h, chloroacetic acid (1.1 g, 11.1 mol) dissolved in 30 mL acetone was added dropwise to the reaction mixture. The reaction mixture was allowed to reflux for 4 h at 60 $^{\circ}$ C. At the end of the reaction, the excessive acetone was removed from the reaction vessel under vacuum, cold water was added, and the organic compound was extracted with ethylacetate (50 mL \times 3). The organic layer was washed with brine solution and dried over Na_2SO_4 . The crude product: 4 was purified by column chromatography using ethylacetate hexane usually 15:85.

4.2.3. General procedure for the synthesis of compounds A1–A9

Compound 4 (0.2 g, 0.6 mol) was dissolved in 30 mL DMSO at room temperature. Triethylamine (0.2 g, 1.9 mol) was added to the reaction mixture. After 1 h, the piperazine containing nucleophile (0.68 mol) dissolved in 10 mL DMSO was added to the reaction mixture. 0.7 g (1.9 mol) HBTU was added to the reaction and the reaction was allowed for regular stirring at room temperature for 24 h. At the end of the reaction, the reaction mixture was poured into ice-water and the organic phase was extracted with ethylacetate (50 mL \times 3). The organic layer was washed with brine solution and dried over Na_2SO_4 . The target compounds obtained were purified using column chromatography with eluting solvents: hexane and ethylacetate usually in 20: 80 ratios.

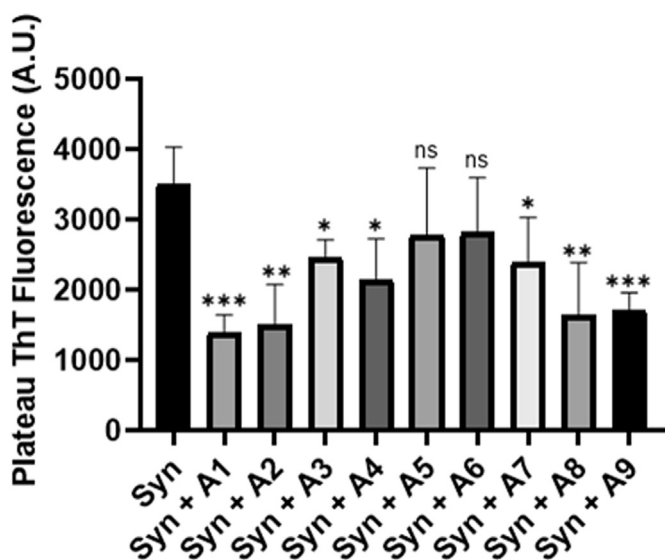


Fig. 5. Final ThT plateau fluorescence for α -syn (control) and α -syn incubated with inhibitors (A1-A9). Here, data represents \pm SEM of fluorescence values from four different wells after reaching plateau phase (≤ 66 h). *** = $p < 0.001$, ** = $p < 0.01$ and * = $p < 0.05$, ns = nonsignificant.

Table 2

ThT fluorescence curve derived values of $t_{1/2}$, t_{lag} , and k_{app} for α -syn and α -syn incubated with inhibitors.

Aggregation reaction	$t_{1/2}$ (h)	t_{lag} (h)	K_{app} ($\times 10^{-3} h^{-1}$)
α -Syn	31.2 ± 0.6	15.1 ± 0.9	108.7 ± 1.8
α -Syn + A1	28.2 ± 0.5	15.9 ± 1.0	128.1 ± 1.7
α -Syn + A2	23.6 ± 1.8	11.6 ± 1.4	144.0 ± 15.0
α -Syn + A3	29.4 ± 0.4	14.1 ± 1.1	118.3 ± 0.7
α -Syn + A4	27.0 ± 0.2	14.4 ± 0.3	120.3 ± 1.2
α -Syn + A5	30.0 ± 1.3	16.1 ± 0.5	116.2 ± 0.7
α -Syn + A6	30.4 ± 1.5	13.9 ± 1.4	121.7 ± 5
α -Syn + A7	29.1 ± 1.3	15.3 ± 0.5	123.2 ± 1.9
α -Syn + A8	27.5 ± 0.6	14.6 ± 0.5	86.6 ± 5.2
α -Syn + A9	28.1 ± 0.2	14.9 ± 0.3	121.3 ± 3.6

4.2.3.1. 1-(4-(7-Chloroquinolin-4-yl)piperazin-1-yl)-2-((5,6-diphenyl-1,2,4-triazin-3-yl)thio)ethan-1-one (A1). Yellow solid, yield = 76% ($R_f = 0.7$ in pure ethylacetate); m.p. 210–212 °C.; 1H NMR (300 MHz, $CDCl_3$) δ 8.75 (d, $J = 4.8$ Hz, 1H), 8.07 (d, $J = 1.5$ Hz, 1H), 7.96 (d, $J = 9.0$ Hz, 1H), 7.62–7.30 (m, 10H), 7.26 (s, 1H), 6.86 (d, $J = 4.8$ Hz, 1H), 4.40 (s, 2H), 3.98 (s, 4H), 3.26 (d, $J = 17.7$ Hz, 4H). ^{13}C NMR (75 MHz, $CDCl_3$) δ 169.53, 166.35, 156.38, 155.87, 154.27, 151.82, 149.99, 135.26, 135.04, 134.98, 131.05, 129.82, 129.30, 128.91, 128.64, 128.53, 126.68, 124.78, 121.77, 109.40, 51.96, 46.24, 42.36, 38.61. LCMS: (ESI, m/z): $[M+H]^+$ calcd. for $C_{30}H_{25}ClN_6OS$ 552.15; found 552.9. Anal. Calcd. for $C_{30}H_{25}ClN_6OS$: C, 65.15; H, 4.56; Cl, 6.41; N, 15.20; O, 2.89; S, 5.80%; found C, 65.35; H, 4.36; Cl, 6.29; N, 15.33; O, 2.68; S, 5.60%.

4.2.3.2. 2-((5,6-Diphenyl-1,2,4-triazin-3-yl)thio)-1-(4-(7-methyl-[1,2,4]triazolo[1,5-a]pyridin-5-yl)piperazin-1-yl)ethan-1-one (A2). Yellow solid, yield = 76% ($R_f = 0.7$ in pure ethylacetate); m.p. 206–208 °C.; ^{13}C NMR (75 MHz, $CDCl_3$) δ 169.39, 166.48, 165.19, 155.96, 154.34, 154.24, 149.88, 134.99, 134.92, 131.07, 129.79, 129.60, 129.28, 128.64, 128.53, 94.85, 47.77, 45.69, 40.89, 33.28, 25.19. LCMS: (ESI, m/z): $[M+H]^+$ calcd. for $C_{28}H_{26}N_8OS$ 522.20; found 523.18. Anal. Calcd. for $C_{28}H_{26}N_8OS$: C, 64.35; H, 5.01; N, 21.44; O, 3.06; S, 6.13%; found C, 64.55; H, 5.31; N, 21.24; O, 3.36; S, 6.00%.

4.2.3.3. 2-((5,6-Diphenyl-1,2,4-triazin-3-yl)thio)-1-(4-tosylpiperazin-1-yl)ethan-1-one (A3). Yellow solid, yield = 76% ($R_f = 0.7$ in pure ethylacetate); m.p. 197–199 °C.; 1H NMR (300 MHz, $CDCl_3$) δ 7.61 (d, $J = 8.1$ Hz, 2H), 7.50 (d, $J = 6.9$ Hz, 2H), 7.47–7.21 (m, 10H), 4.24 (s, 2H), 3.80–3.73 (m, 4H), 3.06 (dd, $J = 27.6, 4.2$ Hz, 4H), 2.41 (s, 3H). ^{13}C NMR (75 MHz, $CDCl_3$) δ 169.35, 166.09, 155.83, 154.22, 144.15, 135.06, 134.92, 132.24, 131.06, 129.89, 129.79, 129.59, 129.31, 128.65, 128.51, 127.73, 67.08, 45.74, 33.33, 21.53. LCMS: (ESI, m/z): $[M+H]^+$ calcd. for $C_{28}H_{27}N_5O_3S_2$ 545.16; found 546.0. Anal. Calcd. for $C_{28}H_{27}N_5O_3S_2$: C, 61.63; H, 4.99; N, 12.83; O, 8.80; S, 11.75%; found C, 61.43; H, 4.79; N, 12.99; O, 8.61; S, 11.96%.

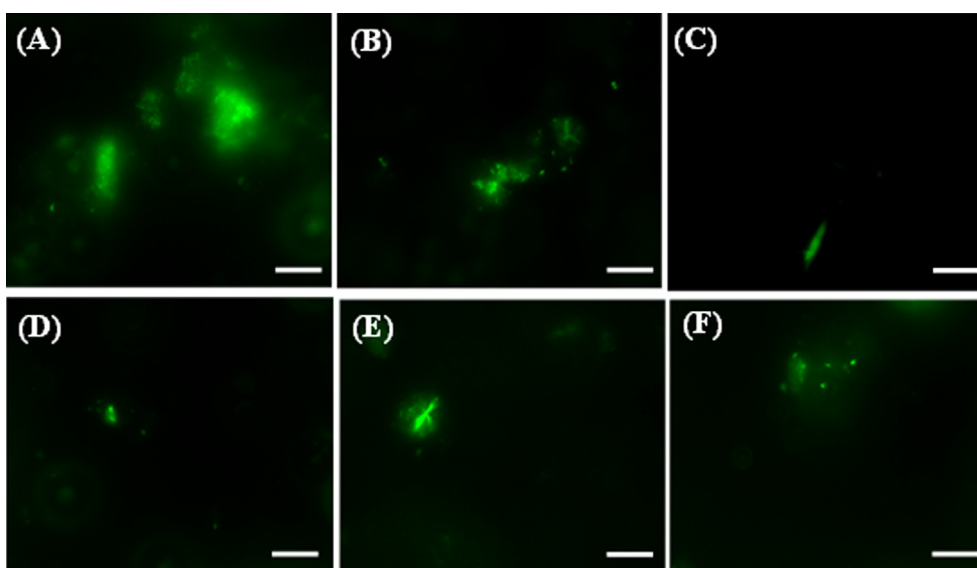


Fig. 6. Representative fluorescence microscopic images of exhibiting the inhibitory effect of compounds A1, A2, A4, A8 and A9 on α -syn aggregation. (A) uninhibited aggregated α -syn. (B–F) α -syn + A1, A2, A4, A8 and A9 respectively. For all microscopic images, all imaging parameters including laser power and zoom level were kept constant. Here, Scale bar represents 10 μ m.

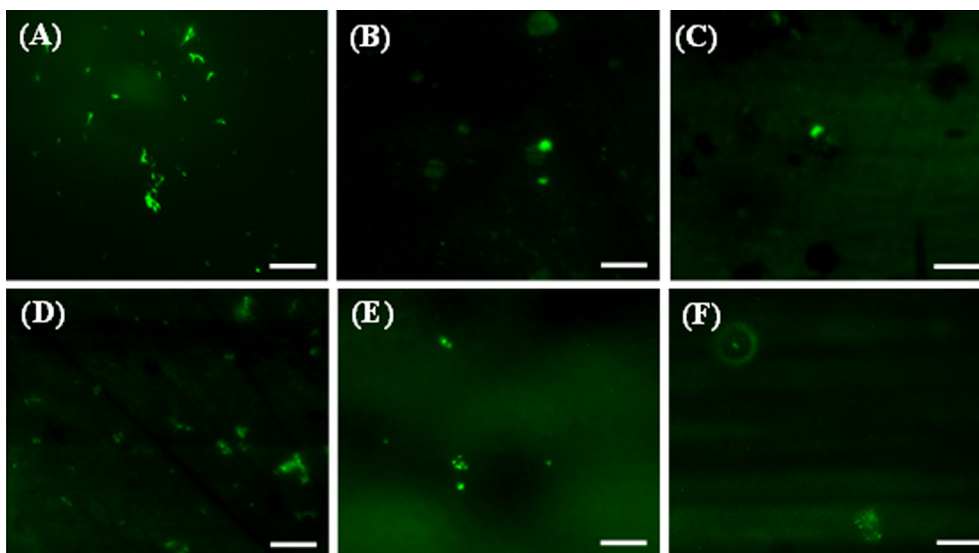


Fig. 7. The representative fluorescence microscopic images showing the disaggregating ability of compounds **A1**, **A2**, **A4**, **A8** and **A9** towards preformed α -syn fibrils. (A) uninhibited aggregated α -syn. (B–F) pre-aggregated α -syn + **A1**, **A2**, **A4**, **A8** and **A9** respectively. For all microscopic images, all imaging parameters including laser power and zoom level were kept constant. Here, Scale bar represents 10 μ m.

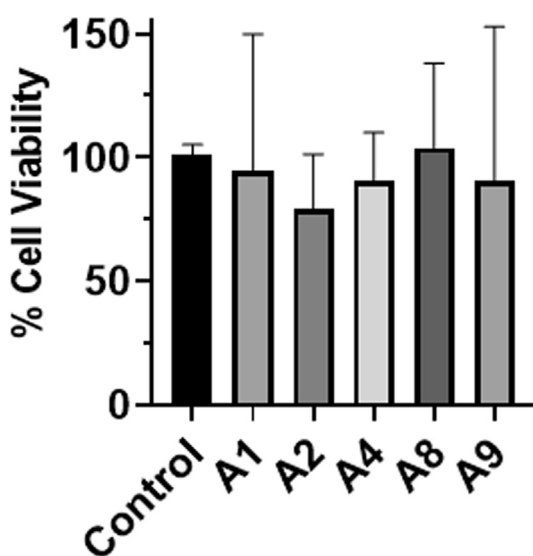


Fig. 8. The % cell viability of Mouse Embryonic Fibroblast cells incubated with compounds (**A1**, **A2**, **A4**, **A8** and **A9**) for 24 h duration. Here, 10 μ M concentration was used for all of the compounds. Data represent \pm SEM of three independent replicates. DMSO was used as a control.

4.2.3.4. 1-(4-((4-Bromophenyl)sulfonyl)piperazin-1-yl)-2-((5,6-diphenyl-1,2,4-triazin-3-yl)thio)ethan-1-one (**A4**). Yellow solid, yield = 76% (R_f = 0.7 in pure ethylacetate); m.p. 223–225 $^{\circ}$ C.; 1 H NMR (300 MHz, $CDCl_3$) δ 7.58 (s, 4H), 7.54–7.13 (m, 10H), 4.23 (s, 2H), 3.75 (d, J = 26.1 Hz, 4H), 3.09 (d, J = 38.4 Hz, 4H). 13 C NMR (75 MHz, $CDCl_3$) δ 166.23, 155.92, 154.27, 135.06, 134.89, 134.46, 132.58, 131.10, 129.80, 129.63, 129.30, 129.13, 128.71, 128.52, 128.41, 67.09, 45.71, 41.67, 38.61. LCMS: (ESI, m/z): $[M+H]^+$ calcd. for $C_{27}H_{24}BrN_5O_3S_2$ 609.05; found 612.0. Anal. Calcd. for $C_{27}H_{24}BrN_5O_3S_2$: C, 53.12; H, 3.96; Br, 13.09; N, 11.47; O, 7.86; S, 10.50%; found C, 53.32; H, 3.76; Br, 13.29; N, 11.66; O, 7.65; S, 10.71%.

4.2.3.5. 2-((5,6-Diphenyl-1,2,4-triazin-3-yl)thio)-1-(4-(naphthalen-2-ylsulfonyl) piperazin-1-yl)ethan-1-one (**A5**). Yellow solid,

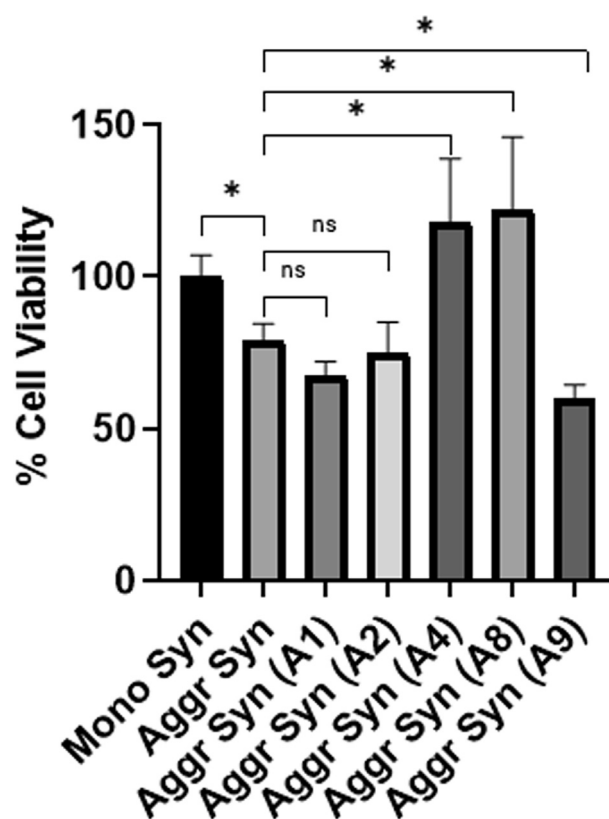


Fig. 9. The % cell viability of MEF (Mouse Embryonic Fibroblast) cells incubated with monomeric α -syn, aggregated α -syn (Aggr Syn) and α -syn aggregated in the presence of compounds (**A1**, **A2**, **A4**, **A8** and **A9**) for 24 h duration. Data represent \pm SEM of three independent replicates. * p < 0.05 and ns nonsignificant.

yield = 76% (R_f = 0.7 in pure ethylacetate); m.p. 231–233 $^{\circ}$ C.; 1 H NMR (300 MHz, $CDCl_3$) δ 8.32 (s, 1H), 7.94 (dd, J = 17.1, 8.1 Hz, 3H), 7.75–7.55 (m, 3H), 7.53–6.99 (m, 10H), 4.21 (s, 2H), 3.75 (dd, J = 9.9, 4.8 Hz, 4H), 3.20 (dd, J = 21.9, 4.8 Hz, 4H). 13 C NMR (75 MHz, $CDCl_3$) δ 169.35, 166.05, 155.75, 154.17, 135.03, 134.91, 132.52, 132.20,

131.00, 129.76, 129.55, 129.43, 129.30, 129.16, 129.10, 128.63, 128.45, 127.99, 127.79, 122.80, 122.67, 67.08, 45.70, 41.71, 33.47. LCMS: (ESI, m/z): $[M+H]^+$ calcd. for $C_{31}H_{27}N_5O_3S_2$: 581.16; found 582.0. Anal. Calcd. for $C_{31}H_{27}N_5O_3S_2$: C, 64.01; H, 4.68; N, 12.04; O, 8.25; S, 11.02%; found C, 64.20; H, 4.48; N, 12.25; O, 8.03; S, 11.22%.

4.2.3.6. 1-(4-((2,4-Dichlorophenyl)sulfonyl)piperazin-1-yl)-2-((5,6-diphenyl-1,2,4-triazin-3-yl)thio)ethan-1-one (A6). Yellow solid, yield = 76% ($R_f = 0.7$ in pure ethylacetate); m.p. 200–202 °C.; 1H NMR (300 MHz, $CDCl_3$) δ 8.04 (d, $J = 2.1$ Hz, 2H), 7.60–7.08 (m, 11H), 4.29 (s, 2H), 3.76 (s, 4H), 3.38 (d, $J = 37.5$ Hz, 4H). ^{13}C NMR (75 MHz, $CDCl_3$) δ 169.34, 166.37, 155.90, 154.30, 137.32, 135.01, 134.91, 133.89, 133.37, 131.77, 131.07, 130.42, 129.79, 129.57, 129.32, 128.63, 128.52, 45.84, 42.24, 38.62, 33.33. LCMS: (ESI, m/z): $[M+H]^+$ calcd. for $C_{27}H_{23}Cl_2N_5O_3S_2$: 599.06; found 602.1. Anal. Calcd. for $C_{27}H_{23}Cl_2N_5O_3S_2$: C, 54.00; H, 3.86; Cl, 11.81; N, 11.66; O, 7.99; S, 10.68%; found C, 54.19; H, 3.65; Cl, 11.62; N, 11.46; O, 7.79; S, 10.98%.

4.2.3.7. 2-((5,6-Diphenyl-1,2,4-triazin-3-yl)thio)-1-(4-((2-nitrophenyl)sulfonyl)piperazin-1-yl)ethan-1-one (A7). Yellow solid, yield = 76% ($R_f = 0.7$ in pure ethylacetate); m.p. 195–197 °C.; 1H NMR (300 MHz, $CDCl_3$) δ 7.58 (s, 4H), 7.54–7.13 (m, 10H), 4.23 (s, 2H), 3.75 (d, $J = 26.1$ Hz, 4H), 3.09 (d, $J = 38.4$ Hz, 4H). ^{13}C NMR (75 MHz, $CDCl_3$) δ 169.35, 166.26, 155.90, 154.30, 148.36, 135.07, 134.92, 134.06, 131.73, 131.06, 130.92, 129.79, 129.55, 129.34, 128.63, 128.52, 124.27, 46.08, 45.69, 42.02, 33.34. LCMS: (ESI, m/z): $[M+H]^+$ calcd. for $C_{27}H_{24}N_6O_5S_2$: 576.12; found 576.9. Anal. Calcd. for $C_{27}H_{24}N_6O_5S_2$: C, 56.24; H, 4.20; N, 14.57; O, 13.87; S, 11.12%; found C, 56.03; H, 4.40; N, 14.78; O, 13.66; S, 11.32%.

4.2.3.8. N-(4-((4-(2-((5,6-diphenyl-1,2,4-triazin-3-yl)thio)acetyl)piperazin-1-yl)sulfonyl)phenyl)acetamide (A8). Yellow solid, yield = 76% ($R_f = 0.7$ in pure ethylacetate); m.p. 222–224 °C.; 1H NMR (300 MHz, $CDCl_3$) δ 7.97 (s, 1H), 7.67 (q, $J = 8.7$ Hz, 4H), 7.53–7.23 (m, 10H), 4.24 (s, 2H), 3.73 (d, $J = 14.7$ Hz, 4H), 3.05 (d, $J = 26.1$ Hz, 4H), 2.19 (s, 3H). ^{13}C NMR (75 MHz, $CDCl_3$) δ 169.35, 166.17, 155.89, 154.27, 143.11, 134.95, 134.81, 131.13, 129.77, 129.62, 129.29, 128.81, 128.65, 128.51, 119.50, 67.06, 46.11, 45.67, 41.66, 33.49, 24.56. LCMS: (ESI, m/z): $[M+H]^+$ calcd. for $C_{29}H_{28}N_6O_4S_2$: 588.16; found 589.0. Anal. Calcd. for $C_{29}H_{28}N_6O_4S_2$: C, 59.17; H, 4.79; N, 14.28; O, 10.87; S, 10.89%; found: C, 59.27; H, 4.58; N, 14.49; O, 10.67; S, 10.69%.

4.2.3.9. N-(4-((4-(2-((5,6-diphenyl-1,2,4-triazin-3-yl)thio)acetyl)piperazin-1-yl)sulfonyl)-2-fluorophenyl)acetamide (A9). Yellow solid, yield = 76% ($R_f = 0.7$ in pure ethylacetate); m.p. 219–221 °C.; 1H NMR (300 MHz, $CDCl_3$) δ 8.79 (s, 1H), 7.64–7.11 (m, 13H), 4.24 (s, 2H), 3.77 (d, $J = 4.5$ Hz, 4H), 3.11 (d, $J = 29.7$ Hz, 4H), 2.23 (s, 3H). ^{13}C NMR (75 MHz, $CDCl_3$) δ 169.36, 168.71, 166.10, 155.85, 154.23, 135.04, 134.90, 131.05, 129.79, 129.56, 129.30, 128.63, 128.51, 127.47, 124.01, 121.34, 115.83, 45.74, 41.66, 38.61, 33.49, 29.68, 24.52. LCMS: (ESI, m/z): $[M+H]^+$ calcd. for $C_{29}H_{27}FN_6O_4S_2$: 606.15; found 607.0. Anal. Calcd. for $C_{29}H_{27}FN_6O_4S_2$: C, 57.41; H, 4.49; F, 3.13; N, 13.85; O, 10.55; S, 10.57%; found C, 57.61; H, 4.29; F, 3.13; N, 13.66; O, 10.32; S, 10.77%.

4.3. Biological screening of the compounds

Luria Bertani Broth, Luria Bertani Broth Agar, Sodium Dodecyl Sulfate (SDS), Cell culture dishes for adherent cells (treated surface) and MTT reagent were purchased from Himedia Laboratories Mumbai, India. DMEM, FBS, Penicillin-Streptomycin, Trypsin-EDTA (0.25%), phenol red and PBS were bought from Gibco. Sodium Azide, Thioflavin-T, Isopropyl Thiogalactoside (IPTG) and DMSO were purchased from Sigma Aldrich, Bangalore, India. The bacterial

Strains *Escherichia Coli* DH5 α and *Escherichia Coli* BL21 (DE3) were purchased from New England Bio Labs, New England. Plasmid pET21a alpha-Syn was obtained as a gift from the Michael J Fox Foundation Hagerstown, USA.

4.3.1. Expression and purification of α -syn protein

E. Coli BL21 (DE3) cells were transformed with pET21a-alpha-synuclein plasmid [28] construct using a calcium chloride method. Transformed *E. Coli* BL21 (DE3) cells containing pET21a-alpha-synuclein plasmid were streaked on LB agar plates containing antibiotic ampicillin (100 μ g/mL). A single colony was used to inoculate into 10 mL overnight cultures in LB medium with ampicillin (100 μ g/mL) at 37 °C, 200 rpm. The overnight culture of transformed *E. Coli* BL21 (DE3) with pET21a-alpha-synuclein was diluted to 100-fold and induced until OD₆₀₀ of 0.4–0.6 for 5 h with 1 mM of IPTG. After the completion of the incubation period, cells were centrifuged at 10,000 g for 30 min at 25 °C. Immediately after centrifugation, cell pellet from 1 L culture was resuspended in 100 mL osmotic shock buffer solution (30 mM Tris-HCl, 40% sucrose and 2 mM EDTA, pH 7.2) and incubated at RT for 10 min. After resuspension, centrifugation at 12,000g for 30 min at 4 °C was done to collect pellet. Then the collected pellet was resuspended in 90 mL cold water with 40 μ L of saturated MgCl₂ and the solution was incubated in ice for 3 min. Further, centrifugation was done at 12,000 g for 30 min at 4 °C. The supernatant collected after centrifugation was adjusted to pH 4 using diluted HCl to precipitate out other proteins. Again centrifugation was done at 12,000 g for 30 min at 4 °C. After centrifugation, the collected supernatant was adjusted to pH 7.4 using 1 M NaOH and loaded into the DEAE-Sephacel matrix to perform anion exchange chromatography. Gradient elution was performed using 50 mM–500 mM NaCl, 20 mM sodium phosphate pH 8.0 to collect desired protein fractions. The various fractions of eluates were pooled and then analyzed by 15% SDS-PAGE and by Western blot using specific antibody such as H3C (Developmental Studies Hybridoma Bank). The desired α -syn protein was further dialyzed against water at 4 °C for 6 h and lyophilized. Lyophilized protein was further used to perform aggregation kinetics.

4.3.2. Preparation of monomeric α -syn

The lyophilized α -syn protein was dissolved in PB (20 mM Sodium Phosphate) buffer, pH 7.4 and then adjusted to pH ~ 11 with 1 M NaOH solution to dissolve preformed aggregates. After 10–15 min, protein dissolved in PB buffer was slowly adjusted to pH 7.4 with 1 M HCl. Then, centrifugation was done at 100,000 g for 1 h at 4 °C to remove preformed aggregate. The supernatant was collected and filtered through a 0.22 μ m filter to remove any particulate matter [41,42]. The concentration of protein was further determined by Nanodrop by measuring the absorbance at 280 nm using the extinction coefficient of 5120 M⁻¹ cm⁻¹ [42].

4.3.3. Aggregation kinetics of α -syn with compounds A1–A9

Thioflavin-T stock (5 mM) was made in PB buffer, pH 7.4 and then filtered through 0.22 μ m filter. Stock of the compounds (A1–A9) was made in DMSO because of their insolubility in aggregation buffer. Aggregation of α -syn has been performed at 37 °C in the aggregation buffer (20 mM sodium phosphate), pH 7.4. Monomeric α -syn (70 μ M) substituted with 20 μ M ThT and 0.01% Sodium Azide was added in 384 wells black flat bottom plate (BRAND) with 3–4 mm glass-beads (sigma) added in each wells. The plate was sealed with transparent film. α -syn (70 μ M) with 10% DMSO was used as a control. For compounds, 1:1 M ratio of compounds (A1–A9) to α -syn was used for determining the inhibition of aggregation. 50 μ L of the sample was added per well. Total four wells have been used for control and each inhibitor. The plate incubated in

Tecan Infinite M200 pro multimode plate reader and real-time aggregation kinetics was monitored in Tecan multiplate reader by ThT fluorescence emission at 485 nm using excitation of 440 nm until plateau phase reached for all compounds and control. Fluorescence emission of ThT was measured every 30 min intervals with orbital shaking of 30 s before every reading. All data were represented as mean \pm standard error of mean (SEM) of four independent replicates.

We further analyzed the ThT fluorescence data by fitting into a sigmoidal curve using the given equation [33]:

$$Y = y_i + m_i t + \frac{y_f + m_f t}{1 + e^{-[(t-t_{1/2})/\tau]}}$$

Here, Y is the fluorescence intensity as a function of time t , y_i and y_f are the intercept of the initial baseline and plateau intensity with the y -axis, m_i and m_f are respective slopes, which are set to zero in our case. $t_{1/2}$ is the time needed to reach half the plateau intensity. τ the elongation time constant was calculated by fitting the data in above equation for each of the four wells and then averaged to reduce unintended bias as explained earlier [33]. The growth of synuclein fibrils was captured by k_{app} , ($=1/\tau$) the apparent rate constant. t_{lag} , time required to nuclei formation was calculated from the intercept between the lag phase and the elongation phase linear extrapolations. Student's t -test was performed to see the statistical difference considering the probability (p) value less than 0.05 using GraphPad Prism 8.0 software.

4.3.4. Fluorescence microscopy

A 10 μ L of the α -syn sample (control) and α -syn incubated with compounds (**A1-A9**) mixed with ThT dye (20 μ M) was transferred to a clean glass slide and covered with a coverslip. After covered with cover slip, extra solution has been wiped with tip of kim wipes to prevent floating of solution. The slide was imaged by Zeiss Axio Observer inverted fluorescence microscope using fluorescein isothio-cyanate filter using 100X (oil immersion) objective. For control and all compounds, laser power and fluorescence intensity has been kept constant.

4.3.5. Disaggregation assay of α -syn in the presence of compounds (A1-A9)

To check the ability of compounds (**A1-A9**) to disaggregate previously formed fibrous species, α -syn incubated as a control and α -syn in the presence of the compounds at 37 $^{\circ}$ C in an incubator for a period of 5 days (**A1, A2, A4, A8 and A9**) in the same molar ratio (1:1) in 384 well Black flat bottom plate (BRAND) and in the absence of ThT. The plate was sealed with sealing tape to prevent evaporation. For disaggregation assay, we used 1 well for control and each compound. Further, after incubation of 5 days, the sample was collected, and fluorescence microscopy has been performed.

4.3.6. Fluorescence microscopy for checking the disaggregation of α -syn in the presence of the compounds (A1, A2, A4, A8 and A9)

To check the disaggregation ability of the compounds (**A1, A2, A4, A8 and A9**), fluorescence microscopy has been performed. Aggregated α -syn sample (control) and aggregated α -syn incubated with compounds (**A1, A2, A4, A8 and A9**) were taken in individual microcentrifuge tubes. Since disaggregation has been performed without addition of ThT. ThT dye (20 μ M) has been added in each sample. After mixing with ThT dye, 10 μ L was transferred to a clean glass slide and covered with a coverslip. After covered with cover slip, extra solution has been wiped with tip of kim wipes to prevent floating of solution. The slide was imaged by Zeiss Axio Observer inverted fluorescence microscope using fluorescein isothio-cyanate filter using 100X (oil immersion) objective. For control and all

compounds, laser power and fluorescence intensity has been kept constant.

4.3.7. Cytotoxicity assay

Mouse Embryonic Fibroblasts (MEFs) cells were allowed to grow in DMEM complete media containing 10% FBS and 1% Penicillin-streptomycin in a humidified CO₂ incubator until they reached around 80% confluency. After reaching confluency, the cells were trypsinized and $2-3 \times 10^5$ cells were added into 96 well transparent clear bottom plate (SPL Lifesciences) and incubated at 37 $^{\circ}$ C in a humidified CO₂ incubator for 24 h. After 24 h of incubation, media was discarded and the test compounds (**A1, A2, A4, A8 and A9**) at a concentration of 10 μ M, monomeric α -syn, aggregated α -syn and aggregated α -syn incubated with **A1, A2, A4, A8 and A9** were added in triplicates and incubated for 24 h. Further, media was removed and MTT reagent (3-(4,5-dimethylthiazol-2-yl)-2,5-diphenyltetrazoliumbromide) (0.5 mg/mL) made in complete media added into cells and incubated for 4 h in dark. After incubation, the media was carefully removed, and formazan crystals were allowed to dissolve in 100 μ L DMSO for 30 min. After 30 min, absorbance has been measured at 570 nm in BioTek SYNERGYH1 (3.04.17) microplate reader. All data were represented as mean \pm standard error of mean (SEM) of three independent replicates. Student's t -test was performed to see the statistical difference considering the probability (p) value less than 0.05 using GraphPad Prism 8.0 software.

Author contributions

MM designed and synthesized all compounds. JG and SG planned experiments for various biophysical assays. JG performed all biophysical assays. PH performed cytotoxicity assays. MM, NH, SG and JG wrote the manuscript.

Declaration of competing interest

The authors declare that they have no known competing financial interests or personal relationships that could have appeared to influence the work reported in this paper.

Acknowledgment

MM is thankful to CSIR for financial assistance in the form of senior research fellowship (SRF). JG is thankful DBT-JRF for Ph.D. fellowship. PH thanks MHRD for Ph.D. Fellowship and additional fellowship during Ph.D. Programme from IIT Gandhinagar. SG acknowledges SERB, Govt. of India (CRG/2018/004960) for partial funding support. We thank Dr. Ishan Raval for his valuable inputs and help with manuscript editing.

Appendix A. Supplementary data

Supplementary data to this article can be found online at <https://doi.org/10.1016/j.ejmech.2020.112705>.

References

- [1] D.W. Dickson, Parkinson's Disease and Parkinsonism: Neuropathology, 2012, pp. 1–16.
- [2] M.G. Spillantini, R.A. Crowther, R. Jakes, M. Hasegawa, M. Goedert, α -Synuclein in filamentous inclusions of Lewy bodies from Parkinson's disease and dementia with Lewy bodies, Proc. Natl. Acad. Sci. U.S.A. 95 (1998) 6469–6473, <https://doi.org/10.1073/pnas.95.11.6469>.
- [3] V.N. Uversky, J. Li, A.L. Fink, Evidence for a partially folded intermediate in α -synuclein fibril formation, J. Biol. Chem. 276 (2001) 10737–10744, <https://doi.org/10.1074/jbc.M010907200>.
- [4] J.R. Mazzulli, F. Zunke, O. Isacson, L. Studer, D. Krainc, α -Synuclein-induced

- lysosomal dysfunction occurs through disruptions in protein trafficking in human midbrain synucleinopathy models, *Proc. Natl. Acad. Sci. Unit. States Am.* 113 (2016) 1931–1936, <https://doi.org/10.1073/pnas.1520335113>.
- [5] J.C. Bridi, F. Hirth, Mechanisms of α -synuclein induced synaptopathy in Parkinson's disease, *Front. Neurosci.* 12 (2018), <https://doi.org/10.3389/fnins.2018.00080>.
- [6] G.A.P. de Oliveira, J.L. Silva, Alpha-synuclein stepwise aggregation reveals features of an early onset mutation in Parkinson's disease, *Commun. Biol.* 2 (2019) 374, <https://doi.org/10.1038/s42003-019-0598-9>.
- [7] M.R. Cookson, The biochemistry of Parkinson's disease, *Annu. Rev. Biochem.* 74 (2005) 29–52, <https://doi.org/10.1146/annurev.biochem.74.082803.133400>.
- [8] J. Madine, A.J. Doig, D.A. Middleton, Design of an N-methylated peptide inhibitor of α -synuclein aggregation guided by solid-state NMR \S , *J. Am. Chem. Soc.* 130 (2008) 7873–7881, <https://doi.org/10.1021/ja075356q>.
- [9] C.R. Fields, N. Bengoa-Vergniory, R. Wade-Martins, Targeting alpha-synuclein as a therapy for Parkinson's disease, *Front. Mol. Neurosci.* 12 (2019), <https://doi.org/10.3389/fnmol.2019.00299>.
- [10] K. Ono, M. Yamada, Antioxidant compounds have potent anti-fibrillogenic and fibril-destabilizing effects for alpha-synuclein fibrils in vitro, *J. Neurochem.* 97 (2006) 105–115, <https://doi.org/10.1111/j.1471-4159.2006.03707.x>.
- [11] R. Kumar, T.S. Sirohi, H. Singh, R. Yadav, R.K. Roy, A. Chaudhary, et al., 1,2,4-triazine analogs as novel class of therapeutic agents, *Mini Rev. Med. Chem.* 14 (2014) 168–207, <http://www.ncbi.nlm.nih.gov/pubmed/24479860>.
- [12] N. Ansari, F. Khodagholi, M. Ramin, M. Amini, H. Irannejad, L. Dargahi, et al., Inhibition of LPS-induced apoptosis in differentiated-PC12 cells by new triazine derivatives through NF- κ B-mediated suppression of COX-2, *Neurochem. Int.* 57 (2010) 958–968, <https://doi.org/10.1016/j.neuint.2010.10.002>.
- [13] H. Irannejad, M. Amini, F. Khodagholi, N. Ansari, S.K. Tusi, M. Sharifzadeh, et al., Synthesis and in vitro evaluation of novel 1,2,4-triazine derivatives as neuroprotective agents, *Bioorg. Med. Chem.* 18 (2010) 4224–4230, <https://doi.org/10.1016/j.bmc.2010.04.097>.
- [14] E. Jameel, P. Meena, M. Maqbool, J. Kumar, W. Ahmed, S. Mumtazuddin, et al., Rational design, synthesis and biological screening of triazine-triazolopyrimidine hybrids as multitarget anti-Alzheimer agents, *Eur. J. Med. Chem.* 136 (2017) 36–51, <https://doi.org/10.1016/j.ejmech.2017.04.064>.
- [15] M. Maqbool, A. Manral, E. Jameel, J. Kumar, V. Saini, A. Shandilya, et al., Development of cyanopyridine-triazine hybrids as lead multitarget anti-Alzheimer agents, *Bioorg. Med. Chem.* 24 (2016) 2777–2788, <https://doi.org/10.1016/j.bmc.2016.04.041>.
- [16] M. Yazdani, N. Edraki, R. Badri, M. Khoshneviszadeh, A. Iraj, O. Firuzi, Multitarget inhibitors against Alzheimer disease derived from 3-hydrazinyl 1,2,4-triazine scaffold containing pendant phenoxy methyl-1,2,3-triazole: design, synthesis and biological evaluation, *Bioorg. Chem.* 84 (2019) 363–371, <https://doi.org/10.1016/j.bioorg.2018.11.038>.
- [17] M. Yazdani, N. Edraki, R. Badri, M. Khoshneviszadeh, A. Iraj, O. Firuzi, 5,6-Diphenyl triazine-thio methyl triazole hybrid as a new Alzheimer's disease modifying agents, *Mol. Divers.* (2019), <https://doi.org/10.1007/s11030-019-09970-3>.
- [18] C.W. Bertoncini, Y.-S. Jung, C.O. Fernandez, W. Hoyer, C. Griesinger, T.M. Jovin, et al., From the Cover: release of long-range tertiary interactions potentiates aggregation of natively unstructured α -synuclein, *Proc. Natl. Acad. Sci. Unit. States Am.* 102 (2005) 1430–1435, <https://doi.org/10.1073/pnas.0407146102>.
- [19] N. Katyal, M. Agarwal, R. Sen, V. Kumar, S. Deep, Paradoxical effect of trehalose on the aggregation of α -synuclein: expedites onset of aggregation yet reduces fibril load, *ACS Chem. Neurosci.* 9 (2018) 1477–1491, <https://doi.org/10.1021/acscchemneuro.8b00056>.
- [20] R.A. Crowther, R. Jakes, M.G. Spillantini, M. Goedert, Synthetic filaments assembled from C-terminally truncated α -synuclein, *FEBS (Fed. Eur. Biochem. Soc.) Lett.* 436 (1998) 309–312, [https://doi.org/10.1016/S0014-5793\(98\)01146-6](https://doi.org/10.1016/S0014-5793(98)01146-6).
- [21] Z. Chi, R. Liu, Y. Teng, X. Fang, C. Gao, Binding of oxytetracycline to bovine serum albumin: spectroscopic and molecular modeling investigations, *J. Agric. Food Chem.* 58 (2010) 10262–10269, <https://doi.org/10.1021/jf101417w>.
- [22] K.V. Sashidhara, R.K. Modukuri, P. Jadiya, K.B. Rao, T. Sharma, R. Haque, et al., Discovery of 3-Arylcoumarin-tetracyclic tacrine hybrids as multifunctional agents against Parkinson's disease, *ACS Med. Chem. Lett.* 5 (2014) 1099–1103, <https://doi.org/10.1021/ml500222g>.
- [23] J. Pan, Z. Ye, X. Cai, L. Wang, Z. Cao, Biophysical study on the interaction of ceftriaxone sodium with bovine serum albumin using spectroscopic methods, *J. Biochem. Mol. Toxicol.* 26 (2012) 487–492, <https://doi.org/10.1002/jbt.21446>.
- [24] P. Ruzza, G. Siligardi, R. Hussain, A. Marchiani, M. Islami, L. Bubacco, et al., Ceftriaxone blocks the polymerization of α -synuclein and exerts neuroprotective effects in vitro, *ACS Chem. Neurosci.* 5 (2014) 30–38, <https://doi.org/10.1021/cn400149k>.
- [25] M. Maqbool, A. Manral, E. Jameel, J. Kumar, V. Saini, A. Shandilya, et al., Development of cyanopyridine–triazine hybrids as lead multitarget anti-Alzheimer agents, *Bioorg. Med. Chem.* 24 (2016) 2777–2788, <https://doi.org/10.1016/j.bmc.2016.04.041>.
- [26] O. Trott, A.J. Olson, AutoDock Vina, Improving the speed and accuracy of docking with a new scoring function, efficient optimization, and multi-threading, *J. Comput. Chem.* 31 (2010) 455–461, <https://doi.org/10.1002/jcc.21334>.
- [27] M. Khoshneviszadeh, M.H. Ghahremani, A. Foroumadi, R. Miri, O. Firuzi, A. Madadkar-Sobhani, et al., Design, synthesis and biological evaluation of novel anti-cytokine 1,2,4-triazine derivatives, *Bioorg. Med. Chem.* 21 (2013) 6708–6717, <https://doi.org/10.1016/j.bmc.2013.08.009>.
- [28] C. Huang, G. Ren, H. Zhou, C. Wang, A new method for purification of recombinant human α -synuclein in Escherichia coli, *Protein Expression and Purification* 42 (2005) 173–177, <https://doi.org/10.1016/j.pep.2005.02.014>.
- [29] W. Hoyer, T. Antony, D. Cherny, G. Heim, T.M. Jovin, V. Subramaniam, Dependence of α -synuclein aggregate morphology on solution conditions, *J. Mol. Biol.* 322 (2002) 383–393, [https://doi.org/10.1016/S0022-2836\(02\)00775-1](https://doi.org/10.1016/S0022-2836(02)00775-1).
- [30] M. Groenning, Binding mode of Thioflavin T and other molecular probes in the context of amyloid fibrils—current status, *J. Chem. Biol.* 3 (2010) 1–18, <https://doi.org/10.1007/s12154-009-0027-5>.
- [31] H. Naiki, K. Higuchi, M. Hosokawa, T. Takeda, Fluorometric determination of amyloid fibrils in vitro using the fluorescent dye, thioflavin T, *Anal. Biochem.* 177 (1989) 244–249, [https://doi.org/10.1016/0003-2697\(89\)90046-8](https://doi.org/10.1016/0003-2697(89)90046-8).
- [32] L.P. Jameson, N.W. Smith, S.V. Dzyuba, Dye-binding assays for evaluation of the effects of small molecule inhibitors on amyloid (A β) self-assembly, *ACS Chem. Neurosci.* 3 (2012) 807–819, <https://doi.org/10.1021/cn300076x>.
- [33] K. Gade Malmos, L.M. Blancas-Mejia, B. Weber, J. Buchner, M. Ramirez-Alvarado, H. Naiki, et al., ThT 101: a primer on the use of thioflavin T to investigate amyloid formation, *Amyloid* 24 (2017) 1–16, <https://doi.org/10.1080/13506129.2017.1304905>.
- [34] A. Kroes-Nijboer, Y.S. Lubbersen, P. Venema, E. van der Linden, Thioflavin T fluorescence assay for β -lactoglobulin fibrils hindered by DAPH, *J. Struct. Biol.* 165 (2009) 140–145, <https://doi.org/10.1016/j.jsb.2008.11.003>.
- [35] W.M. Pardridge, The blood-brain barrier: bottleneck in brain drug development, *NeuroRx* 2 (2005) 3–14, <https://doi.org/10.1602/neurorx.2.1.3>.
- [36] T. Bohnacker, A.E. Prota, F. Beaufils, J.E. Burke, A. Melone, A.J. Inglis, et al., Deconvolution of Buparlisib's mechanism of action defines specific PI3K and tubulin inhibitors for therapeutic intervention, *Nat. Commun.* 8 (2017) 14683, <https://doi.org/10.1038/ncomms14683>.
- [37] F. Beaufils, N. Cmiljanovic, V. Cmiljanovic, T. Bohnacker, A. Melone, R. Marone, et al., 5-(4,6-Dimorpholino-1,3,5-triazin-2-yl)-4-(trifluoromethyl)pyridin-2-amine (PQR309), a potent, brain-penetrant, orally bioavailable, pan-class I PI3K/mTOR inhibitor as clinical candidate in oncology, *J. Med. Chem.* 60 (2017) 7524–7538, <https://doi.org/10.1021/acs.jmedchem.7b00930>.
- [38] F. Cheng, W. Li, Y. Zhou, J. Shen, Z. Wu, G. Liu, et al., admetsAR: a comprehensive source and free tool for assessment of chemical ADMET properties, *J. Chem. Inf. Model.* 52 (2012) 3099–3105, <https://doi.org/10.1021/ci300367a>.
- [39] Y.H. Zhao, M.H. Abraham, A. Ibrahim, P.V. Fish, S. Cole, M.L. Lewis, et al., Predicting penetration across the blood-brain barrier from simple descriptors and fragmentation schemes, *J. Chem. Inf. Model.* 47 (2007) 170–175, <https://doi.org/10.1021/ci600312d>.
- [40] V.M.S. Gil, N.C. Oliveira, On the use of the method of continuous variations, *J. Chem. Educ.* 67 (1990) 473, <https://doi.org/10.1021/ed067p473>.
- [41] J. Pujols, S. Peña-Díaz, M. Conde-Giménez, F. Pinheiro, S. Navarro, J. Sancho, et al., High-throughput screening methodology to identify alpha-synuclein aggregation inhibitors, *Int. J. Mol. Sci.* 18 (2017), <https://doi.org/10.3390/ijms18030478>.
- [42] X. Meng, L.A. Munishkina, A.L. Fink, V.N. Uversky, Effects of various flavonoids on the alpha-synuclein fibrillation process, *Parkinson's Dis.* 2010 (2010) 1–16, <https://doi.org/10.4061/2010/650794>.